Journal of Metals, Materials and Minerals, Vol. 32, No. 1, pp. 65-71, 2022

Effects of milling time on sintering properties and formation of interface Al_4C_3 on graphite reinforced Al-4.5Cu-1.5Mg nanocomposite

Angga Khairul FAHMI[1], Haris RUDIANTO[2,*], Agus Sukarto WISMOGROHO[2], Wahyu Bambang WIDAYATNO[2], Didik ARYANTO[2], and Bambang HERMANTO[2]

[1] *Advance Materials Laboratory, Departement of Mechanical Engineering, Gunadarma Univesity, Jl. Margonda Raya No. 100, Depok, West Java, 16424, Indonesia*

[2] *Research Center for Physics, National Research and Innovation Agency, Setu, South Tangerang, Banten, 15314, Indonesia*

***Corresponding author e-mail:** harisrudianto@staff.gunadarma.ac.id

Received date:
3 May 2021
Revised date
28 January 2022
Accepted date:
30 January 2022

Keywords:
Alumunium;
Graphite;
Nanocomposite;
Shaker mill;
Sintering

Abstract

Aluminum-based metal matrix nanocomposites have been extensively researched and developed for aerospace and automotive applications. Al-4.5Cu-1.5Mg with 0.5 wt% graphite were milled for 2 h, 4 h, 6 h, and 8 h using shaker mill under argon gas. The phenomena of deformation, fracturing, and cold welding during shaker mill were investigated to observe how the shaker mill effects on their morphology and formation of intermetallic phases due to its very high speed. Sintering under ultra-high purity argon gas for 99.9999% was done to produce high density materials. Intermetallic phase Al_4C_3 was found as a result reaction between aluminum and graphite during milling. Formation of Al_4C_3 is very important to the alloy as an interface between matrix and reinforcement particle in order to have higher hardness. A decrease in Peaks Cu and followed by an increase in Al_2Cu precipitation in the XRD pattern occurred with increasing milling time. The role of Al_2Cu precipitation is very important in improving mechanical properties, resulting in the highest hardness value reaching 97 HV and a density value of 83% at 8 h of milling.

1. Introduction

Improving mechanical performance of the materials used in the aircraft and automotive industries has always been the focus of many research groups in the related fields [1]. Aluminum-based metal matrix composites (Al-MMCs) are widely used for these kind of applications because of their high strength to weight ratio [2]. Particularly, AA 2024 with copper as the main alloying element (3.8 wt% to 4.9 wt%) has been used extensively to produce aircraft, shaft and gear fittings for industrial applications owing to its high fatigue resistance [3,4].

The study of aluminum-based metal matrix with graphite reinforcement particle is a combination of materials that have the potential to meet these industries requirements because of their higher mechanical properties leading to increasing efficiency [5]. MMC aluminum will exhibit improved mechanical properties and best performance when graphite reinforcing particles are homogeneously distributed with the right volume graphite fraction in the aluminum matrix [6]. Formation of interface of aluminum carbide Al_4C_3 was heavily investigated by many researchers in the field of carbon-based reinforced aluminum matrix nanocomposites. Al_4C_3 was used as an interface to transfer the stress from the matrix to reinforcement leading to higher mechanical properties of the nancomposites. But, manufacturing process to produce interface Al_4C_3 remains a challenge because it needs long period of time to produce it.

The miling process greatly affects the results of the distribution of reinforcement in the matrix. The longer milling time will result in a significant reduction in particle size with a high degree of homogenization. However, the difference in energy and force received by the powder during the grinding process can override the milling time. In previous studies by S.E. Hernández-Martinez *et al.*, investigation on the effects of milling techniques on the properties of AA2024-ZrO_2 powder showed that the shaker mill method was the most effective method to produce nanocomposites with superior mechanical properties [7]. During shaker mill of AA2024-ZrO_2, particle reinforcement was dispersed homogeneously, the level of formation of the interface between matrix and particle reinforcement is greater, and agglomeration does not occur [7]. In this study, shaker mill was used to produce graphite reinforced Al-4.5Cu-1.5Mg matrix nanocomposite. The effects of shaker mill process to powder morphology, sintering properties and intermetallic phase formation were investigated.

2. Experimental method

Al-Cu-Mg is mixed elementary as a matrix mixture with graphite as the reinforcing particle. Table 1 and Figure 1 show the composition and morphology of the particles. Dry mixing for 2 h, 4 h, 6 h, and 8 h with ball to powder ratio of 10:1 using the PPF-UG stainless steel shaker mill at the Department of Physics, Indonesian Institute of

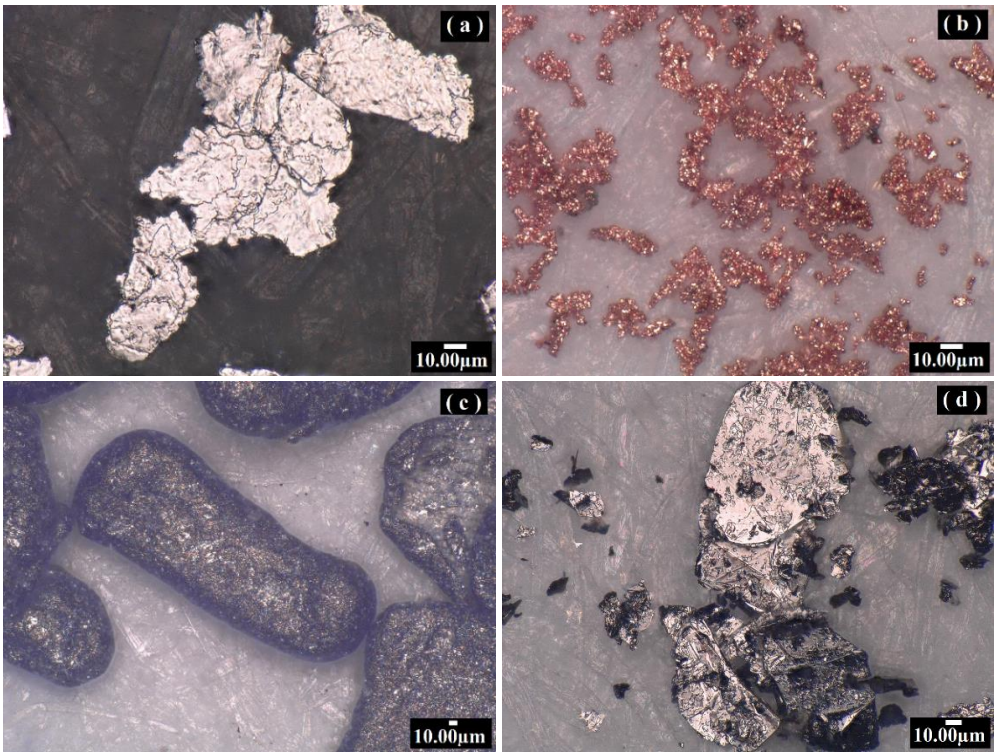

Figure 1. Micrograph of particle shape of raw matériels used in this research, (a) alumunium, (b) copper, (c) magnesium, and (d) graphite.

Table 1. Chemical Compositions.

Elements	Al	Cu	Mg	Gr
Compotitions (wt%)	93.5	4.5	1.5	0.5

Science was done. Ultra-high purity argon gas for 99.9999% during milling was used to prevent unnecessary reaction. After shaker mill, the powder was stored inside atmosphere and pressure-controlled box to prevent exposure to room atmosphere leading to oxidation reaction.

For compaction process, 1.5 wt% stearate acid as a lubricant was added to the powder to produce green body materials and to reduce ejection force in order to pull out the materials from the mold easily. Sintering under ultra-high purity argon gas for 1 h at a heating rate of 10°C·min^{-1} was carried out to produce high density materials. Sintering density was calculated using Archimedes method according to ASTM B 328 standard. The phenomena that occur in powders after milling and sintering were analyzed.

Thermal analysis test under argon gas with a heating rate of 10°C·min^{-1} using Differential Scanning Calorimetry (DSC) by Setaram LabSys Evo was done from 20°C to 700°C to analyze the thermal properties. Morphology of the particles and microstructures were characterized using optical microscopy by Keyence VHX-6000 and Scanning Electron Microscope-Energy Dispersive Spectroscopy (SEM-EDS) by Hitachi SU-3500. X-Ray Diffraction (XRD) by Rigaku-Smartlab 3kV for determining phase composition, especially for identifying intermetallic phases before and after sintering. Micro Vickers hardness uses the MicroMet® 5100 Series with a load of 300 gf.

3. Results and discussion

3.1 Powder characterizations

Figure 2 shows the mmorphology of the powder after milling at various times. The powder immediately undergoes significant changes after 2 h of milling. Milling time greatly affects changes in particle shape, particle size, and homogeneity. At 4 h of milling, the particles still look similar as in 2 h of milling. However, at 6 h of milling the particle size began to show a huge decrease in size, it can be seen that many small particle sizes have been formed even though there are still some particles that look big. It is very different after 8 h of milling, the direct particles are dominated by small and uniform sizes and have the smallest particle size compared to other milling times. This indicates that longer milling time will lead to finer particles.

The reinforcement particles in the nanocomposite not only act as a medium to improve mechanical properties but also act as a medium to assist in the milling process so that nanocrystalline attainment can quickly be formed. This has also been confirmed by previous research conducted by J. L. Hernandez R *et al.* [8], graphite is not only a reinforcing particle but also plays an active role in helping reduce particle size because of its function as a process control agent in achieving steady conditions or conditions where particles are no longer experiencing reduction size. This was also revealed in another study by Fogagnolo *et al.* [9]. In AA 6061 which was milled using a high-energy planetary ball mill, the powder had deformation and turned flat after 6 h of milling and became irregular after 24 h. When 5% of AlN reinforcement particles were added, the powder turned irregular in a shorter time of 10 h.

Another factor that affects the change in particle size in the manufacture of nanocomposites is the type of milling used. Each type of milling has its characteristics with different finishes. In previous research conducted by S. E. Hernandes *et al.* [7] on AA7075 + 2 wt% ZrO_2, nanocomposite particles turned flat using a Planetary Ball Mill. In contrast to the types of milling Horizontal Attritor Mill and Shaker Mill. In the Horizontal Attritor Mill, powder particles begin to lead

to an irregular shape, although some particles are still flat but thicker when compared to particles produced by the Planetary Ball Mill. In the shaker mill results, the overall shape of the particles becomes irregular. In terms of the homogeneity of the reinforcement, shaker mill produces excellent particle dispersion, in contrast to the other two methods that are still clustered, even the size of the reinforcement particles is still large.

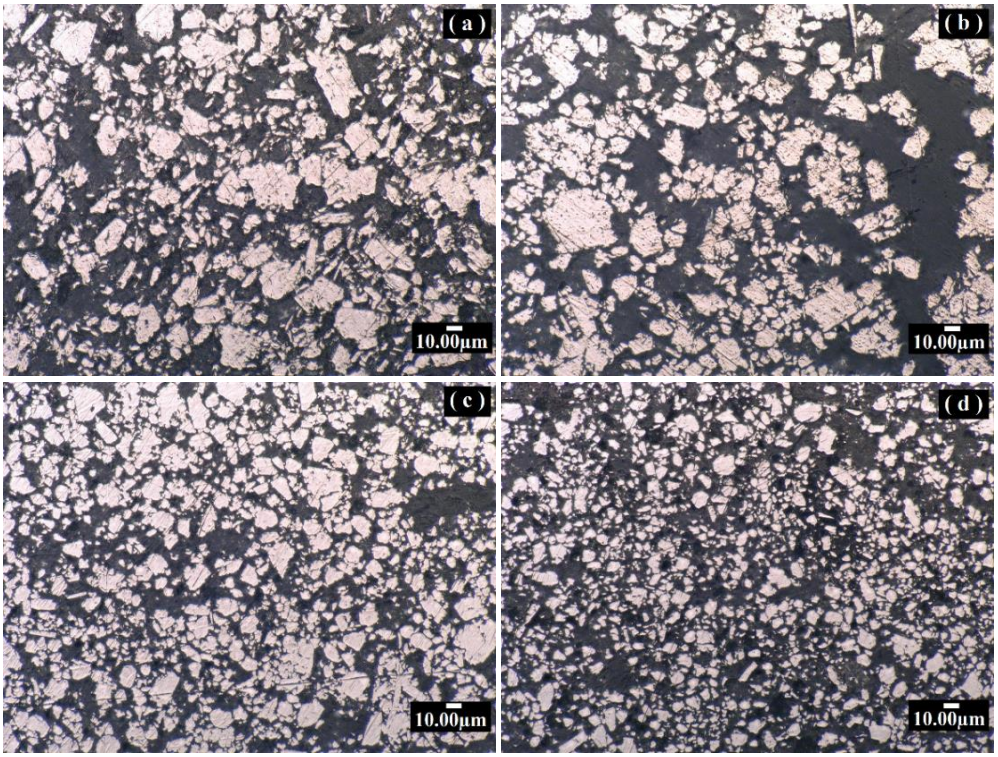

Figure 2. The microstructure of the powder after various milling times with 0.5 wt% graphite, (a). 2-h, (b). 4-h, (c). 6-h, and (d). 8-h.

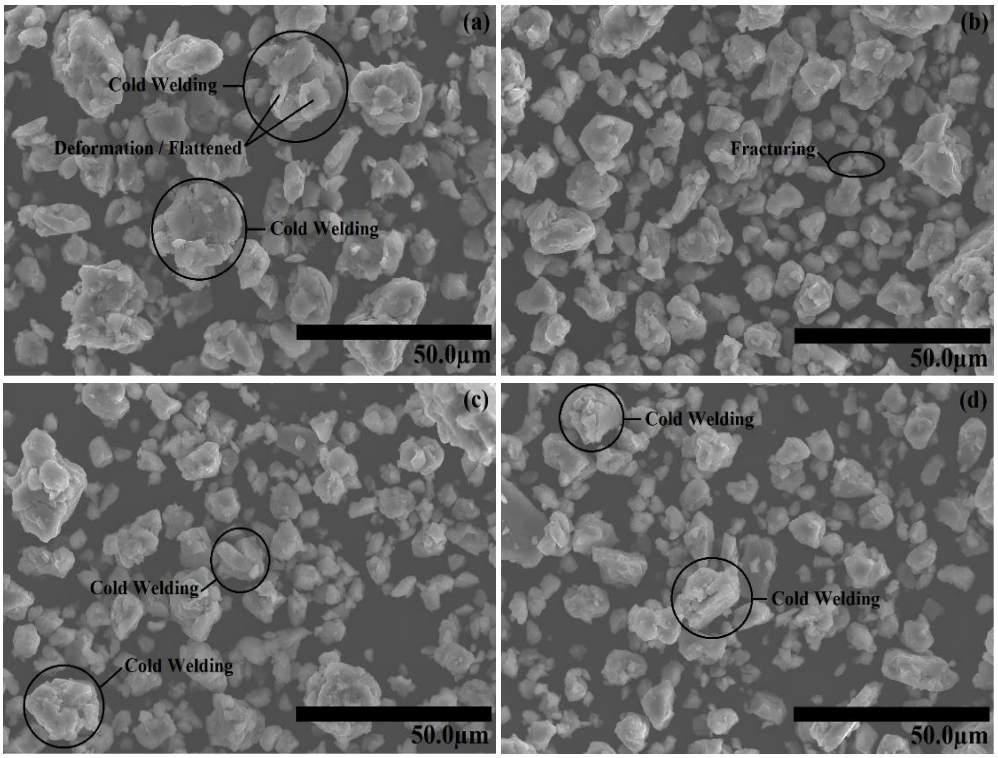

Figure 3. Morphology evolution of Al 4.5Cu-1.5Mg + 0.5 wt% Graphite after Shaker Mill using SEM (a) 2 h milling, (b) 4 h milling, (c) 6 h milling, and (d) 8 h milling.

Figure 3 is the powder morphology after various milling times. During the milling process, the ball-to-ball and ball-to-wall collisions allow each particle to experience three phenomena that occur, namely deformation, fracturing, and cold welding. These particles will experience destructive damage to change the original shape of each component (deformation) which causes damage and changes in particle size (fractures). The particles that have been crushed will weld to each other which leads to an increase in size (cold welding) so that each new particle is formed with various arrangements of each initial element. This phenomenon is continuous and recurring during milling [10-12].

Figure 4 shows the XRD patterns of the powder after milling and sintering. The powder after 2 h of milling shows that Cu content is still clearly visible as element, it begins to disappear at 4 h of milling, and so on. The disappearance of elemental Cu content at 4 h and so on is assumed that Cu dissolved into the aluminum matrix by forming Al-Cu intermetallic compound. When sintered, the sample gets heat energy which can help the Al-Cu reaction so that it forms Al_2Cu as a new compound, as in the XRD pattern after sintering shows an increase in the Al_2Cu peak at 2 h milling. But in for 6 h and 8 h milled after sintering materials, the Al_2Cu intensity experienced a decrease. High energy milling with increasing time allows Cu content to be dissolved and nanosized so that the formation of Al_2Cu peaks in the XRD pattern will decrease after sintering due to its very fine size and dispersion on the matrix [13,14].

Graphite as a reinforcement particle in this composition has a role that can help in the nanosized process during milling, as a hard and brittle material that allows graphite to more easily undergo fracture during milling so that it becomes nanoscale faster. With nanoscale size, graphite will react with the aluminum matrix and form fine carbide/Al_4C_3 as in the results of other authors' research on Al with various types of Carbon, especially with a small amount of 0.5 wt% [14]. In Figure 4, Al_4C_3 is formed after milling and after sintering with small peaks. The presence of Al_4C_3 is a very important intermetallic compound in aluminum-carbon nanocomposites because of its strength interfacial bond. But in other cases, the formation of Al_4C_3 is generally destructive due to its poor corrosion resistance and brittleness. But in other cases, Al_4C_3 has an important role in increasing the hardness value of the aluminum matrix. Brittle Al_4C_3 can change soft aluminum so that it can withstand great forces and wear resistance [15,18]. Another carbide formed is Fe_3C. Fe content appears as an impurity due to the impact of the ball-to-ball or ball-to-jar collision force during milling to produce small Fe particles. The presence of Fe content during milling makes it react with graphite and form new compounds. However, Fe is an advantageous impurity because of its properties that can increase the hardness value in aluminum-carbon nanocomposite.

Figure 5 shows a DSC graph on an 8-h powder milling. Two endothermic peaks and one exothermic peak occurred. The first endothermic peak occurs at a temperature of 450°C, this peak is assumed to be eutectic reaction of Al-Mg [18]. At a temperature of 550°C, in previous studies, the eutectic peak of Al-Cu was supposed to appear, but this peak did not appear because it was closed off the exothermic peak formed before 550°C. The second endothermic peak has a high enough intensity that occurs at 641°C, this peak is assumed to be the melting point of the Al matrix. Several researchers show slightly different melting temperature with similar to AA2024 chemical compositions. The difference in the melting point of Al occurs due to differences in variations in the milling process. It was found that melting temperature decreased as the milling time increased, it is assumed that with finer powder morphology leads to speed up the diffusion process during sintering [8,19,20].

The exothermic peak shows at 567°C with high intensity. This peak is an oxidation reaction (Al_2O_3) that occurs. With 4 times higher of the thermal expansion coefficient of aluminum (27.4×10^{-6}/°C) compared to alumina (7.4×10^{-6}/°C), it will produce Gibbs energy so that the oxide layer can be easily destroyed due to internal pressure which results in the aluminum expansion (reach for melting) with increasing temperature during processing. If observed, exothermic peaks appear before melting al, so that when the highest point is exothermic (cracking oxide), the graph immediately falls free to form an endothermic peak (melting of aluminum) [19].

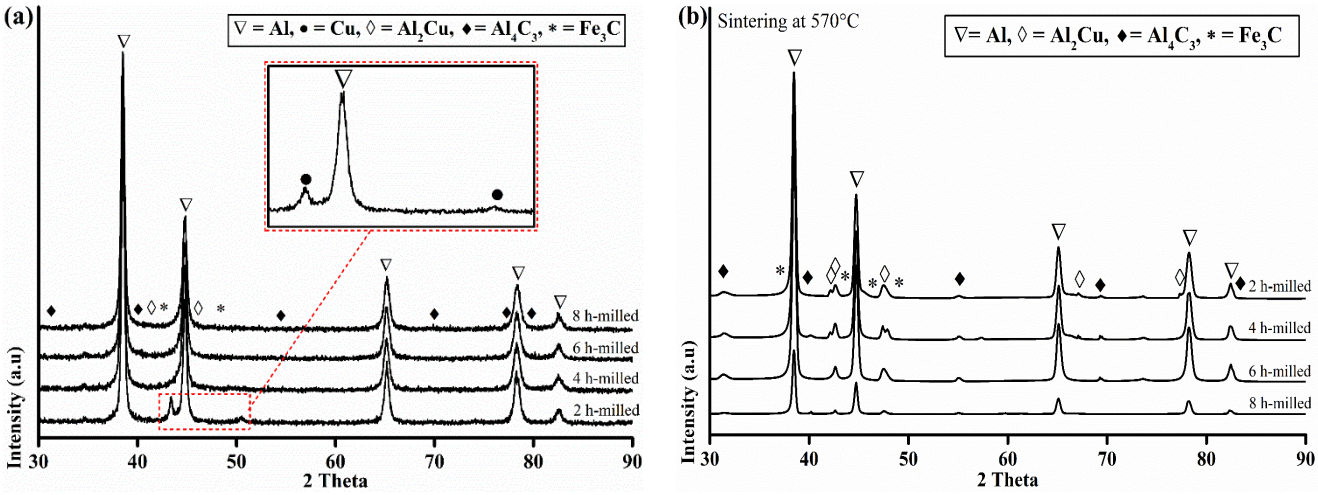

Figure 4. XRD graphs, (a) after milling, and (b) sintering.

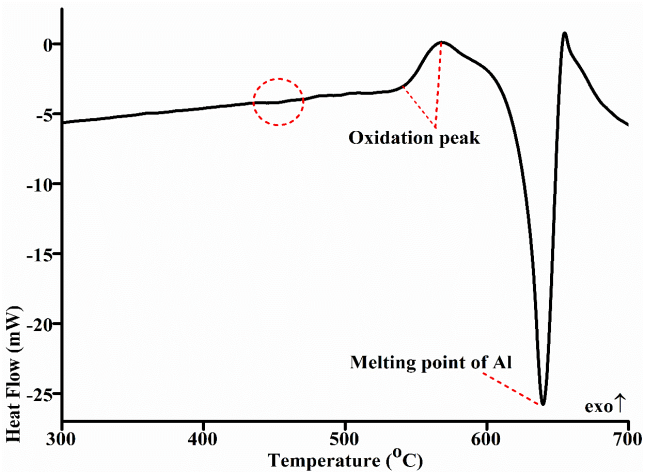

Figure 5. DSC curva of powder after milling during 8 h.

The oxides do often appear on the outer layer of aluminum powder. This oxide layer is very damaging and inhibits the particle diffusion process during sintering which causes it to be not optimal in obtaining the sintering density. In the sintering process, DSC can be used to estimate the optimum sinter temperature. The sintering temperature must be close to the melting point of the matrix so that the highest exothermic peak (567°C) can be determined as the optimum sintering temperature and will be proven in the results of the sintering properties [18]. The study of effects of magnesium on sintering of aluminum powder has been done intensively by R. N. Lumley *et al.* and T. Pieczonka *et al.* They showed that magnesium has very important role on removing of oxide layer on aluminum particles. Magnesium will react with oxide layer Al_2O_3 at lower temperature and form spinel ($MgAl_2O_4$). The addition of 1.5 wt% Mg in this mixture is expected to have enough to remove the oxide layer [21,22].

3.2 Sintering properties

Figure 6 shows the values of density and hardness of micro Vickers on this nanocomposite with variations in temperature and milling time. In Figure 6(a) and 6(c), it shows that 570°C gives highest hardness and sintering density for 97 Vickers Hardness respectively. Higher sintering density leads to higher hardness. According to DSC graph shown by Figure 5, at 570°C is expected to have some liquid phases from elements or compound which have lower melting point such as Al-Mg or Al-Cu. These liquid phases also play important role to obtain high density by filling the pores during sintering, this mechanism is called liquid phase sintering. But at 580°C and 590°C sintering density decreased which leads to having lower hardness. At these temperatures, it is expected grain growth occurred will lead to having bigger pore which is called Ostwald Ripening phenomena [16,21,22].

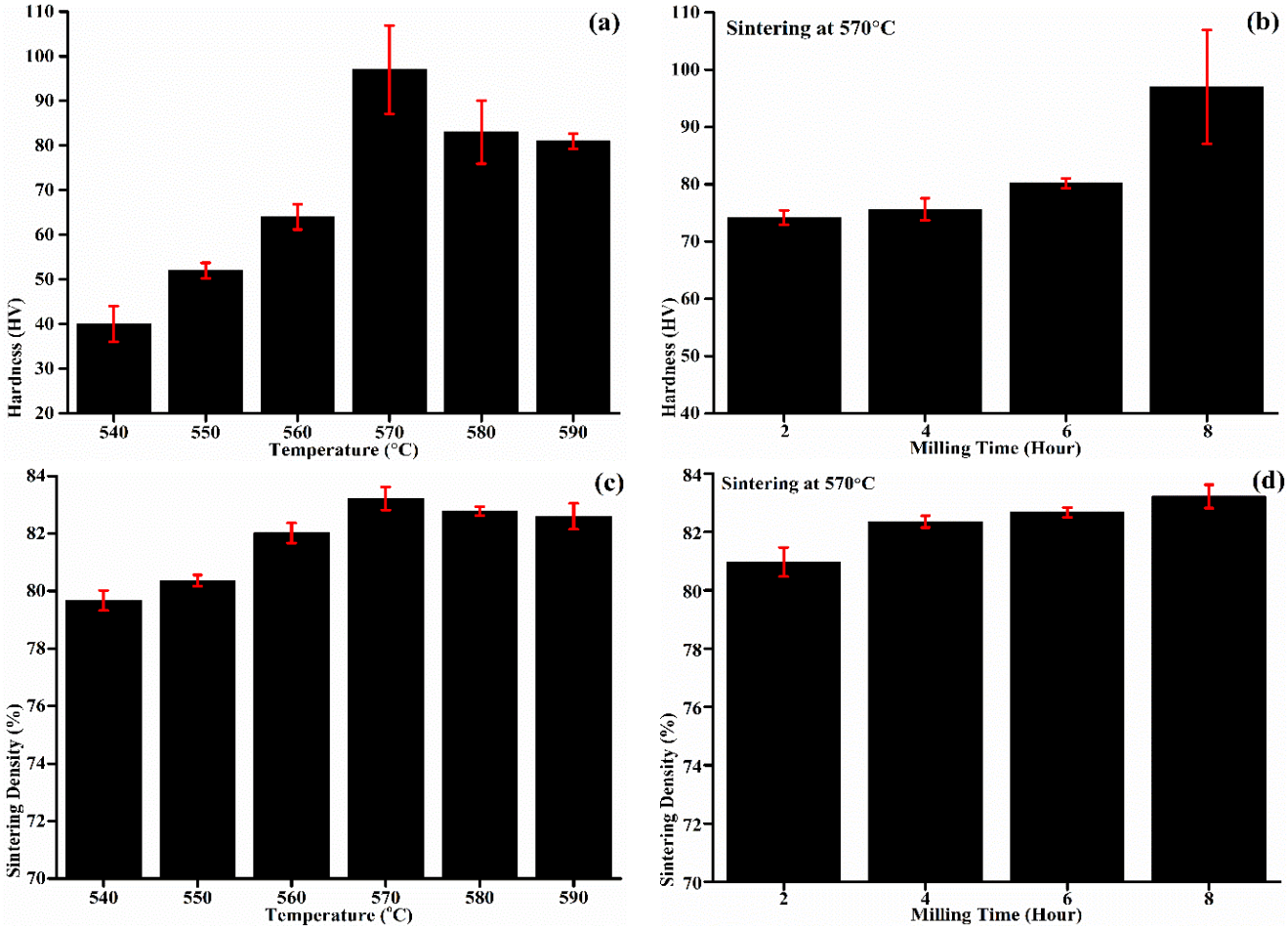

Figure 6. Graph of hardness and sintering density, (a) (c) hardness and sintering density with differences in sintering temperature, and (b) (d) hardness and sintering density with differences in milling time.

In Figure 6(b) and 6(d), it shows the effects of milling time on hardness. With a long milling time, it causes a high degree of deformation, reducing the grain size to a level where the nanoparticles formed will be well distributed and form aluminum-carbide (Al_4C_3) as an interface between the matrix and the reinforcement particles. Fine powder will have bigger surface area that will react faster at elevated temperature and this helps during sintering of the nanocomposite. Heat energy during the sintering process allows nanoparticles to diffuse and can increase the grain boundary volume. Under these conditions, the dissolved atoms replace the solvent atoms within the grain boundaries. The fast separation of atoms from one grain to another leads to rapid homogenization and results in the formation of a new intermetallic compound (Al_4C_3) which serves to resist deformation when gaining forces [23].

Figure 7 shows the SEM-EDS images after sintering at a temperature of 570°C with a milling time of 8 h which is the optimum variables for this nanocomposite. The images of SEM shows that there are several colors with different shapes and sizes. The aluminum matrix as the main element is marked in gray. If observed, there are two other colors, namely dark gray and light gray. Light gray represents Cu and Mg elements characterized by dark gray [8]. on the EDS point analysis, it is proven that weight to percent (Table 2) on each element mentioned has a high percentage compared to other points, for example at point 3 which is an element of rich Cu based on literature and previous research proved on EDS point analysis by having a high wt% compared to point 2 and other points, as well as the Mg element in the EDS point analysis.

During the milling process, the phenomena of fracture and cold-welding lead to uniformity in the distribution of each element. On the light ash color, it forms a rich Cu precipitate due to the heat energy received during the sintering process, allowing it to form Al_2Cu deposits [10]. It seems as expected that magnesium is dissolved around grain boundary of aluminum and close to pore due its reaction with aluminum oxide layer to form $MgAl_2O_4$. This formation will help diffusion process between particles during sintering leading to high density materials [24]. The graphite as a particle reinforcement in this nanocomposite is appeared as carbon on EDS Mapping Analysis that is homogenously dispersed. Carbon based materials such as graphene, graphite and CNT is usually found around grain boundary of the matrix. This leads to assume that shaker mill is able to produce homogenously dispersed reinforcement particles.

Table 2. The EDS results correspond to the point locations shown in Figure 7.

Point	wt%			
	Al	Cu	Mg	Graphite
1	88.71	01.16	00.94	09.20
2	94.79	04.26	00.94	-
3	69.97	28.95	01.07	-
4	96.22	01.92	01.86	03.30

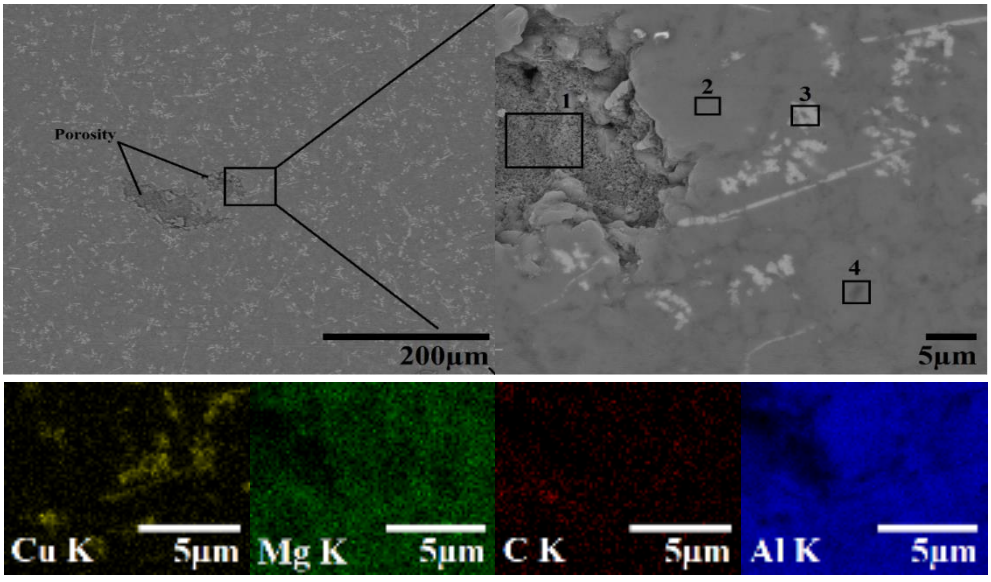

Figure 7. SEM-EDS results after sintering with a milling time of 8 h at 0.5 wt% Gr.

4. Conclusions

Shaker mill technique has successfully produced homogenously dispersed Al-4.5Cu-1.5Mg with 0.5 wt%. Longer shaker mill process increase homogeneity and produce finer nanocomposite powder. It seems 8 h shaker milling time and 570°C sintering temperature under argon gas are suitable variable for this nanocomposite which showing highest sintering density and hardness for 83% relative and 97 Vickers Hardness respectively. Intermetallics Al_2Cu and Al_4C_3 were found after shaker mill and sintering as results from high energy milling. Fe_3C was found as impurities in this nanocomposite shown by XRD pattern. This was expected to form as a high energy collision between stainless steel ball and jar or ball to ball.

Acknowledgements

This research was supported and funded by the Indonesian Institute of Science Physics Research Center (LIPI-Puspiptek) and Gunadarma University.

References

[1] R. Pérez-Bustamante, M. J. González-Ibarra, J. González-Cantú, I. Estrada-Guel, J. M. Herrera-Ramírez, M. Miki-Yoshida, and R. Martínez-Sánchez, "AA2024-CNTs composites by milling process after T6-temper condition," *Journal of Alloys and Compounds*, vol. 536S, pp. S17-S20, 2012.

[2] H. Ahamed, and V. Senthilkumar, "Consolidation behavior of mechanically alloyed aluminum based nanocomposites reinforced with nanoscale Y_2O_3/Al_2O_3 particles," *Materials Characterization*, vol. 62, pp. 1235-1249, 2011.

[3] P. Kumar H. G., and A. Xavior M., "Assessment of mechanical and tribological properties of Al 2024-SiC-Graphene hybrid composites," *Procedia Engineering*, vol. 174, pp. 992-999, 2017.

[4] A. Xavior, M. P. Kumar H. G, and A. Kumar. K, "Tribological studies on AA 2024-Graphene/CNT nanocomposites processed through Powder metallurgy," *Materials Today: Proceedings*, vol. 5, pp. 6588-6596, 2018.

[5] ASM Handbook Volume 2: Properties and selections: Nonferrous alloys and special-purpose materials, United States of America: ASM International, 1990.

[6] L. Ceschini, A. Morri, and F. Rotundo, "Forming of metal matrix composites," *Comprehensive Materials Processing*. Bologna: Elsevier pp. 159-186, 2014.

[7] S. E. Hernández-Martinez, J. J. Cruz-Rivera, C. G. Garay-Reyes, R. Martínez-Sánchez, I. Estrada-Guel, and J. L. Hernández-Rivera, "Comparative study of synthesis of AA 7075-ZrO_2 metal matrix composite by different mills," *Journal of Alloys and Compounds*, vol. 643, pp. S107-S113, 2015.

[8] J. L. Hernandez R., J. J. Cruz R., C. Gomez Y, O. Coreno A., and R. Martınez-Sanchez, "Synthesis of graphite reinforced aluminum nanocomposite by mechanical alloying," *Materials Transactions*, vol. 51, no. 6, pp. 1120-1126, 2010.

[9] J. B. Fogagnolo, F. Velasco, M. H. Robert, and J. M. Torralba, "Effect of mechanical alloying on the morphology, micro-structure and properties of aluminium matrix composite powders," *Materials Science and Engineering A*, vol. 342, pp. 131-143, 2003.

[10] A. Alizadeh, M. Maleki, and A. Abdollahi, "Preparation of super-high strength nanostructured B_4C reinforced Al-2Cu aluminum alloy matrix composites by mechanical milling and hot press method: Microstructural, mechanical and tribological characterization," *Advanced Powder Technology*, vol. 28, pp. 3274-3287, 2017.

[11] S. F. Tikhov, K. R. Valeev, A. N. Salanov, S. V. Cherepanova, N. N. Boldyreva, V. I. Zaikovskii, V. A. Sadykov, D. V. Dudina, O. I. Lomovsky, V. E. Romanenkov, and E. E. Pyatsyushik, "Phase formation during high-energy ball milling of the 33Al-45Cu-22Fe (at%) powder mixture," *Journal of Alloys and Compounds*, vol. 736, pp. 289-296, 2018.

[12] A. Santos-Beltrán, V. Gallegos-Orozco, R. Goytia Reyes, M. Miki-Yoshida, I. Estrada-Guel, and R. Martínez-Sánchez, "Mechanical and microstructural characterization of dispersion strengthened Al-C system nanocomposites," *Journal of Alloys and Compounds*, vol. 489, no. 2, pp. 626-630, 2010.

[13] J. B. Fogagnolo, D. Amador, E. M. Ruiz-Navas, and J. M. Torralba, "Solid solution in Al-4.5 wt% Cu produced by mechanical alloying," *Materials Science and Engineering A*, vol. 433, pp. 45-49, 2006.

[14] C. Dhadsanadhep, T. Luangvaranunt, J. Umeda, and K. Kondoh, "Fabrication of Al/Al_2O_3 composite by powder metallurgy method from aluminum and rice husk ash," *Journal of Metals, Materials and Minerals*, vol.18 (2), pp. 99-102, 2008.

[15] W. Xu, W. Chenchong, Z. Zhichao, L. Ping, S. Yanhua, and Z. Guofu, "Interfacial microstructure and growth mechanism of Al_4C_3 in Gr_f/Al composites fabricated by liquid pressure method," *Micron*, vol. 65, pp. 10-14, 2014.

[16] H. Rudianto, S. S. Yang, Y. J. Kim, and K. W. Nam, "Sintering behavior of hypereutectic aluminum-silicon metal matrix composites powder," *International Journal of Modern Physics: Conference Series*, vol. 6, pp. 628-633, 2012.

[17] J. Wang, L. N. Guo, W. M. Lin, J. Chen, C. L. Liu, S. D. Chen, S. Zhang, and T. T. Zhen, "Effect of the graphene content on the microstructures and properties of graphene/aluminum composites," *New Carbon Materials*, vol. 34, no. 3, pp. 275-285, 2019.

[18] A. Gökçe, F. Findik, and A. O. Kurt, "Sintering and aging behaviours of Al-4Cu-XMg PM alloy," *The Canadian Journal of Metallurgy and Materials Science*, vol. 55, no. 4, pp. 391-401, 2016.

[19] Z. Y. Liu, T. B. Sercombe, and G. B. Schaffer, "The effect of particle shape on the sintering of aluminum," *Metallurgical and Materials Transactions A*, vol. 38A, pp. 1351-1357, 2007.

[20] M. Wu, Y. Liu, Z. Zeng, and W. Luo, "Effect of temperature on deformation behavior of sintered porous AA2024 during semisolid compression," *The Minerals, Metals & Materials Society*, vol. 69, no. 4, pp. 763-769, 2017.

[21] R. N. Lumley, T. B. Sercombe, and G. M. Schaffer, "Surface oxide and the role of magnesium during the sintering of aluminum," *Metallurgical and Materials Transactions A*, vol. 30, pp. 457-463, 1999.

[22] T. Pieczonka, Th. Schubert, S. Baunack, B. Kieback, "Dimensional behavior of aluminum sintered in different atmospheres," *Materials Science and Engineering A*, vol. 478, no. 1-2, pp. 251-256, 2008.

[23] C. Suryanarayana, "Mechanical alloying and milling," *Progress in Materials Science*, vol. 46, pp. 1-184, 2001.

[24] H. Rudianto, G. J. Jang, S. S. Yang, Y. J. Kim, and I. Dlouhy, "Effect of SiC particles on sinterability of Al-Zn-Mg-Cu P/M alloy," *Archives of Metallurgy and Materials*, vol. 60, no. 2, pp. 1383-1385, 2015.